Combustion synthesis and development of Ti–O–C aluminium composites

Krzysztof Naplocha *

Institute of Production Engineering and Automation, Wroclaw University of Technology, ul. Łukasiewicza 5, 50-371 Wroclaw, Poland

ARTICLE INFO

ABSTRACT

Aluminium matrix composite reinforced with Ti compounds was successfully fabricated by SHS combustion synthesis and squeeze casting course. Prepared samples from mixture containing Ti, C and Al_2O_3 fibres were heated in microwave reactor to ignite synthesis and produce porous preform for subsequent infiltrating with liquid metal. Studies showed that synthesizing temperature has been remarkably increased by applying higher magnetron power and addition of graphite. Synthesis of specimens prepared from preliminary ball milled Ti and C powders proceeded at the highest propagation wave velocity. Microwave heating of metal Ti powder in the stream of CO_2 resulted in formation of corrugated precipitates composed of titanium oxide with carbon inclusions $TiO(C)$ and Ti_2O_3. The produced preforms were impregnated by squeeze casting with the aluminium alloy AlSi7Mg. Proper interface with slight reduction of Ti oxide between the reinforcement and the matrix was developed. Subsequently, the samples were annealed at 500 and 1000 °C. Annealing at the lower temperature induced creation of $Ti_3O_2(C)$ and Al_2O_3. This process was continued at 1000 °C, and additionally some $Ti(Al_{0,8}Si_{0,2})_3$ pellets appeared in the matrix. With prolonged annealing, oxygen was completely removed from Ti compound and oval grains of $Ti(C)$ were created, enveloped with Al_2O_3. In the matrix, larger and numerous Ti_3AlSi_5 pellets were formed. Hardness examination showed that the best strengthening effect was achieved after annealing at 1000 °C.

© 2011 Elsevier B.V. All rights reserved.

1. Introduction

Carbides or oxycarbides attract wide interest because of their unique physical properties such as high hardness, corrosion and oxidation resistance at elevated temperatures, good thermal and electrical conductivity, low reactivity and high melting point [1–3]. However, due to their low fracture toughness, they reveal small resistivity to thermal shocks and usually require introducing additional components. Saturating a porous ceramic preform with ductile matrix may improve its resistance to initiation and propagation of cracks in various ways. Nowadays, variable methods of manufacturing ceramic skeletons and their subsequent impregnating with liquid alloys are elaborated and developed.

High-temperature synthesis SHS activated with microwaves, presented in [4] as MACS (microwave activated combustion synthesis), enables producing porous preforms to be reinforced with composite materials. Microwave heating improves the process as well as affects structure and conversion degree of the initial substrates mixture. Benefits of using microwaves or plasma have been already confirmed several times [5,6].

In the case of dielectric materials, the penetrating microwaves generate mainly internal electric field. It puts electrons or ions in oscillation and makes dipoles rotate. Striking elastically and rubbing each other they generate heat. The first parameter that determines ability of microwave absorption is the dielectric loss factor ε'' (very small for Al_2O_3 and TiO_2).

Falling radiation on non-ferromagnetic metals (Ti and Al) with solid compact structure, induces currents in macroscale, which in turn create opposed field blocking and reflecting microwaves. However, if the metal is in form of particles covered with insulating oxides, penetration of microwaves can be observed and the arising currents heat-up the material in microscale. The tangent component of magnetic field created by microwave radiation induces electric field in the particle skin, which thickness for metals is usually a 0.1–10 μm.

For fine metallic powders, the skin significantly affects heating of a particle core, especially that penetration depth increases with temperature [7]. The currents induced in this layer can change magnetic properties, even of paramagnetic materials (Al, Ti). In [8], the loss factor coefficients were determined on the ground of the Mie–Lorenz theory. It was found that with increasing thickness δ (more precisely r/δ ratio) the dielectric loss factor ε'' decreases dozens times, whereas coupling with the magnetic field becomes most intensive and the magnetic loss factor μ'' reaches its maximum at some average value of this ratio (r/δ = ca. 20).

The concept accepted in this work consists in impregnating a porous preform of hard and brittle material with a relatively ductile aluminium alloy. The Al_2O_3 fibres should enhance initial strength

* Tel.: +48 71 3204236.
  E-mail address: krzysztof.naplocha@pwr.wroc.pl

Table 1
Specimens composition with maximum combustion temperature T_m and wave velocity v.

Specimen symbol	Composition [vol%]			T_m [°C]		v [cm/s]
	Al_2O_3	Ti	C	at 250 W	at 500 W	
A10T5	10	5	–	1250	–	–
A10T10	10	10	–	1360–1410	1560–1660	–
A10T10C5	10	10	5	1400–1480	1840–1960	0.22–0.29
A10T10C10	10	10	10	–	1560–1670	0.18–0.26
A10TC15	10	15		–	1410–1540	0.32–0.43

of the preform, whereas the Ti powder is converted to hard carbides and oxides. Microwave heating of powdered mixture is a relatively new area of research. To gain insight into the phenomena that occur inside reactor chamber with heated material a detailed study of absorption power distribution was performed. Microwave first heats skin of paramagnetic Ti powder and subsequently partly dielectric Ti–O compound. This permits to ignite and support SHS synthesis of solid components with flowing CO_2 gas. Constructed reactor and developed method is an innovative way to heat materials, both ceramic and metal.

2. Experimental

Powders provided by AlfaAesar company and Saffil fibres were used for production of the preforms. Average size of Ti and C particles amounted to 44 μm (−325 mesh), whereas diameter of fibres (96% Al_2O_3 +4% SiO_2) ranged between 4 and 6 μm. Specimens were prepared by a three-step process: production of preforms by SHS synthesis, squeeze casting infiltration and thermal annealing. In the first stage, proper quantities of powders and fibres were mixed for 15 min with 3% water solution of silica binders to obtain homogeneous mixture. Next, the mixture of powders and fibres was drained-off and formed to rectangular preforms 6 × 4 × 1 cm. Volume fractions amounted to 5–10% of Ti powder and to 5–10% of graphite. Simplified symbols informing about volume fractions of Al_2O_3 fibres (A), titanium (T), and graphite (C) were established (Table 1). For example, the specimen A10T10C5 contained 10% of Al_2O_3, 10% of Ti and 5% of C (all percentages volumetric). Specimens with symbol TC were prepared of Ti and C powders comminuted in a ball mill for 14 h. The milling process was performed under argon atmosphere in an attritor containing hard steel balls of 11 mm in diameter. The following operation parameters: ball to powder ratio (BPR) = 20:1; rotational speed = 80 rpm were used.

The prepared preforms were heated-up in microwave field in order to ignite the combustion synthesis and to process the components with flowing CO_2. The specially designed microwave furnace comprised a rectangular waveguide, a chamber
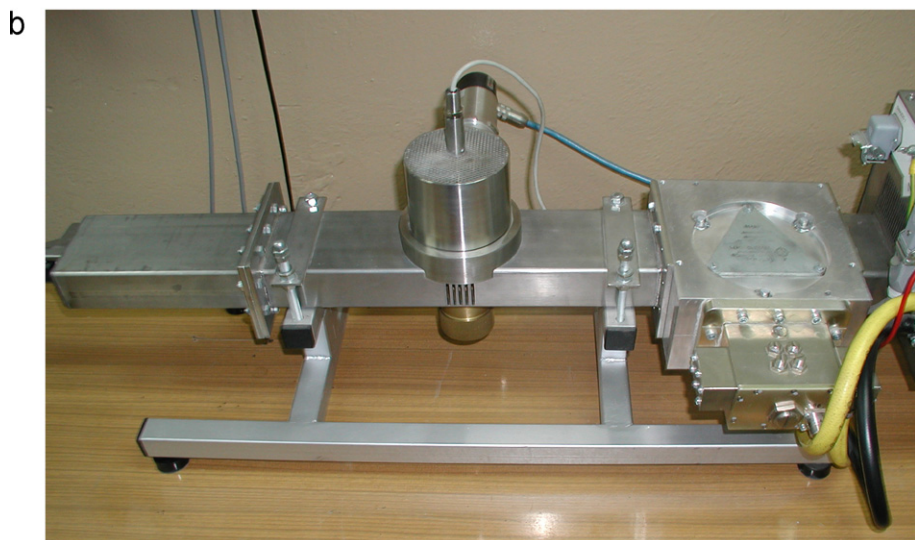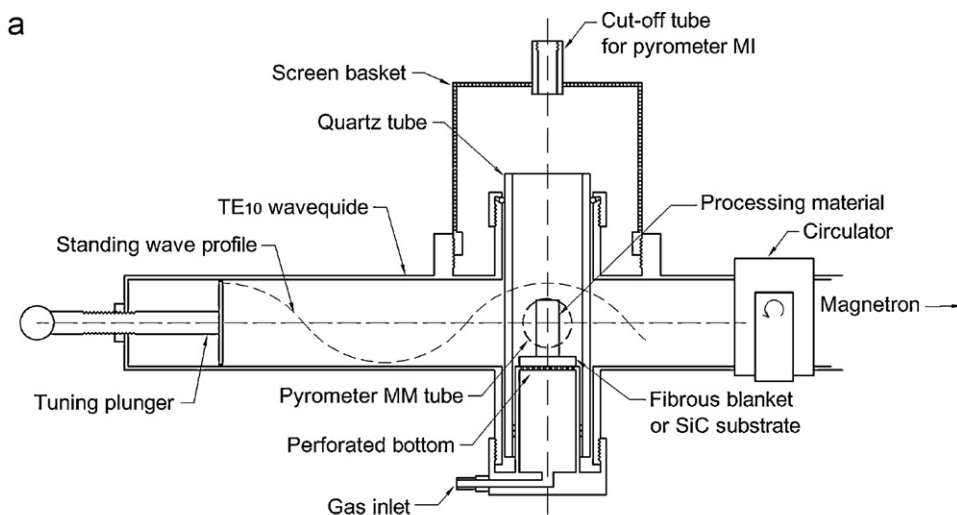

Fig. 1. (a) Diagram of single mode microwave reactor, and (b) a photograph of the reactor with circulator to protect 2.45 GHz magnetron.
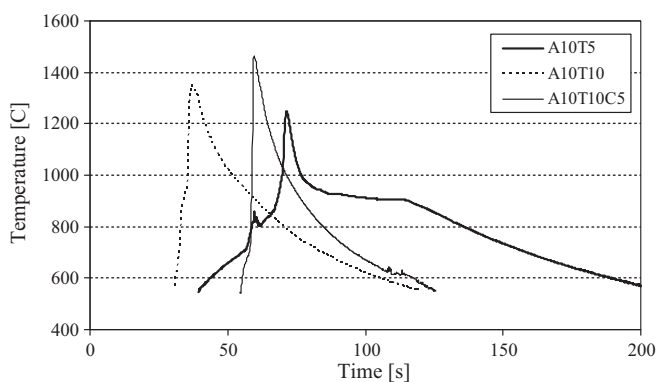
Fig. 2. Synthesis temperature profiles of the A10T5, A10T10 and A10T10C10 specimens heated with microwave power of 250 W.

Fig. 4. Proposal of the reaction mechanism of the carbothermal reduction during SHS synthesis.

with quartz tube and ended with a tuner, see Fig. 1. Processed material placed in chamber on perforated bottom can be insulated with fibrous blanket or to intensify heating on SiC substrate strongly absorbing microwave radiation. Position of processed specimens, determined experimentally, coincides with the node of an electric field in a standing wave. The microwave power was maintained during throughout the whole synthesis. Temperature was measured with a pyrometer Raytek, model Marathon MM, with temperature range from 500 to 3000 °C and with detected spot dia. 0.6 mm. Measuring beam was directed at the centre of the specimen side wall. Velocity of combustion synthesis was controlled by the camera through the slot on the front of waveguide or by using pyrometer with integrated through-the-lens video sighting. To support synthesis, the magnetron was supplied with 250–500 W power.

The preforms were infiltrated with the aluminium alloy EN-AC AlSi7Mg by direct squeeze casting. Hot-work tool steel mould was mounted in 60-tonne hydraulic press. The major parts of the mould, i.e. the die and the punch were preheated to 300 °C and 200 °C, respectively. The prepared preforms were preheated to ca. 500 °C and then, shortly before pouring, were placed in the die. Molten metal was poured and then almost immediately, pressure of 40 MPa was applied and kept for 10–20 s during solidification. In order to remove all gases from porous perform mould was vented.

Annealing of composite specimens was performed under protective atmosphere of argon with 5% of H_2 as a reducing agent. Structures were examined with an optical microscope and a scanning microscope Hitachi S-3400 N equipped with a microanalyser EDS. Phase identification was carried out using an X-ray diffractometer Rigaku Ultima IV with Cu Kα radiation at 40 kV and 40 mA, and using ICDD (2008) cards.

3. Results and discussion

3.1. SHS synthesis of preforms

Microwave heating of the materials that react and change their physical properties is a complex process. In a prepared preform
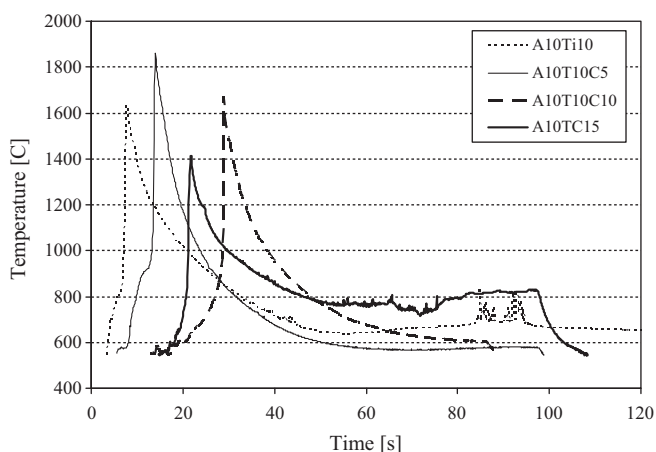
based on alumina fibres almost transparent for microwaves and surface-heated Ti particles, combustion synthesis was ignited and supported. The performs were heated-up in their entire volume, although due to concentration of microwaves on the preform wall, synthesis started at its top surface and moved down along with a typical propagation front.

The adiabatic synthesis temperature is directly influenced by enthalpy of the product formation. Considering the simplest variant of synthesis course, the relationship is:

$$Ti(s) + 2CO_2(g) \rightarrow 2CO(g) + TiO_2(s) - 381\ kJ \qquad (1)$$

Amount of the released heat energy is relatively large and should allow a self-propagating synthesis. On the other hand, flowing gas chills specimens and too large distance between the reactants may lead to ceasing the reaction as it was observed in the preforms containing 5% Ti (A10T5). Thus, to support the propagation front, this specimen was heated-up with on a SiC substrate. Then the temperature reached 1250 °C, see Fig. 2, and after the main synthesis stage stayed stable at about 900 °C due to absorption of microwave energy by the created reaction products.

With Ti content increased to 10% in the A10T10 specimens, it was possible to run the self-sustaining synthesis with use of a

Fig. 3. Synthesis temperature profiles of the A10T10, A10T10C5, A10T10C10 and A10TC15 specimens heated with microwave power of 500 W.

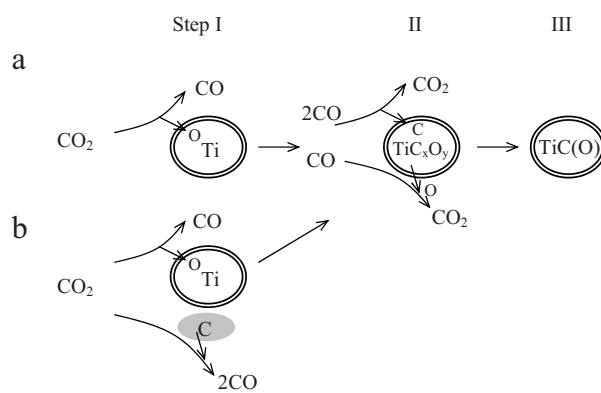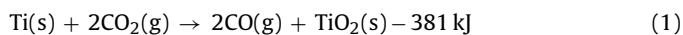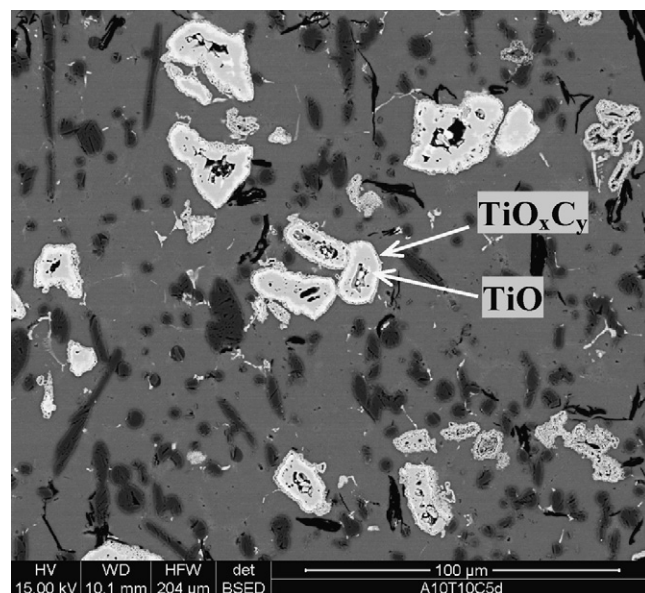**Fig. 5.** Partly reacted Ti particles with large voids inside and jagged envelope around them.
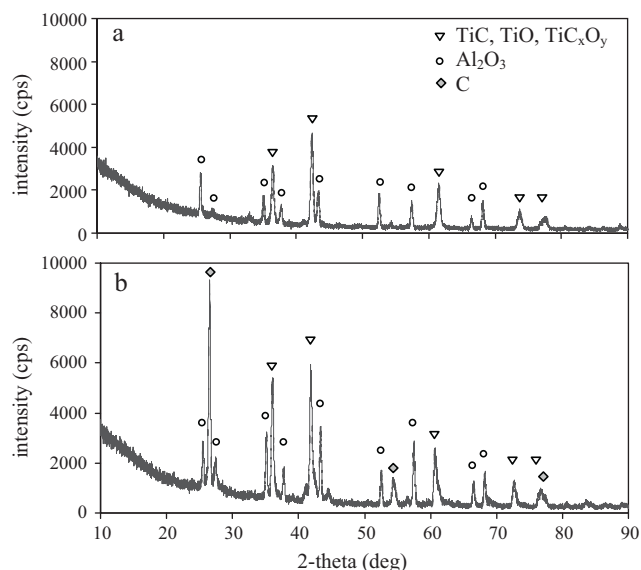
Fig. 6. (a) XRD patterns of A10T10, and (b) A10T10C10 specimens.

Fig. 8. Microstructure with EDS analysis of composite reinforced with the A10TC15 preform.

250 W magnetron. Maximum temperature ranged between 1360 and 1410 °C. Addition of 5% C increased the temperature to ca. 1400–1480 °C. In both series A10T10 and A10T10C5, when the propagation front passed, the specimens relatively quickly cooled down below the minimum temperature of the pyrometer measuring range (550 °C).

In all the recorded temperature curves, before the main synthesis stage, slight fluctuations at about 900 °C were observed, see Figs. 2 and 3. This could evidence transformation of α-Ti to β-Ti, that is present in the binary system at 882 °C. Then, although the pyrometer did not record the so high temperature, probably fusion of Ti particles proceeded, as well as transport of oxygen and its dissolution in the particles. In the researches of combustion Ti in air [9,10] it was found that the reaction kinetics depended on oxygen adsorption. Concentration of oxygen increased linearly to finally form Ti_2O_3.

Higher power of the magnetron allowed higher maximum synthesis temperatures for the specimens A10T10 and A10T10C5 of 1560–1670 °C and 1840–1960 °C, respectively. Moreover, after the propagation front passed, the temperature remained at constant level of 600–700 °C, see Fig. 3. In some cases, temporary temperature jumps could be observed on this plateau, what evidenced that microwaves initiated reaction of the unprocessed residues. Especially in the case of the A10TC15 specimens, the primary reaction
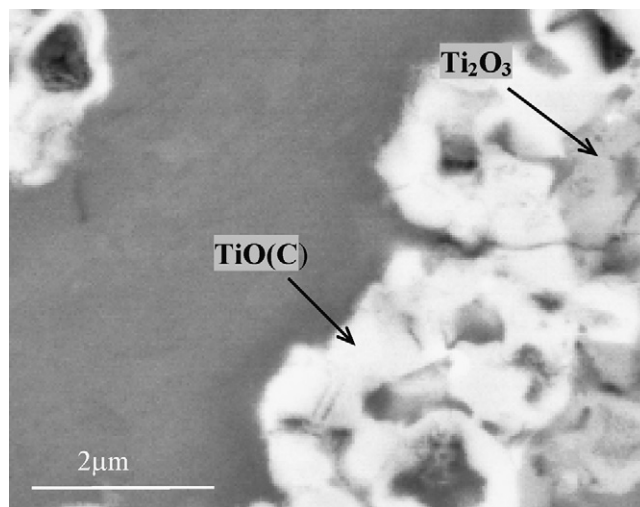
stage was followed by slow temperature increase to 800–820 °C and then the reaction was continued for ca. 1 min at 830–900 °C. For these specimens, the synthesis temperature was the lowest and usually did not exceed 1500 °C. On the other hand, their synthesis proceeded at the highest propagation wave velocity of 0.32–0.43 cm/s. Increase of graphite content from 5 to 10% in the A10T10C10 specimens also did not enhance the synthesis temperature that reached 1560–1670 °C at the lowest wave velocity of 0.18–0.26 cm/s. It should be noted, that usually at lower velocity conversion degree of product is higher.

In the presented research, CO_2 reacts on Ti surface and in some specimens also on C flakes, see Fig. 4 step I. Graphite contributes to increase of the amount of CO important for synthesis and to absorption of microwave energy due to high loss factor. The reaction course

$$C(s) + CO_2(g) \rightarrow 2CO(g) + 113 \, kJ \tag{2}$$
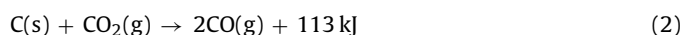
involves a temperature decrease, so at higher C content of 10% the synthesis temperature is lower in comparison with the preforms containing 5% C, see Fig. 3. The effect of graphite could be even more significant when energy is absorbed by the synthesis products. More defective graphite structure, containing impurities and mixed with other components, intensely absorbs microwaves. This could be the reason why instantaneous temperature changes occurred after the propagation front passed during synthesis of the A10TC15 specimens containing milled Ti and C powders.
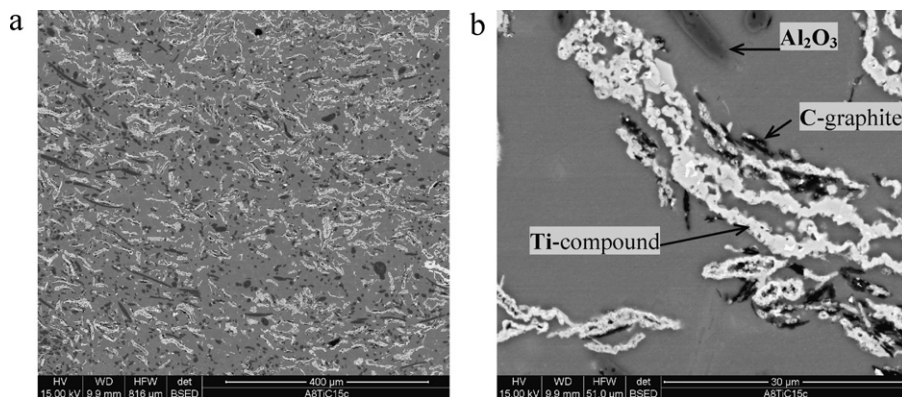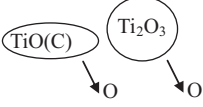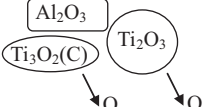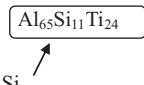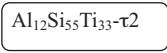

Fig. 7. (a) BSE image of composite reinforced with the A10TC15 preform, and (b) Ti compound with adhering C flakes in aluminium alloy matrix.

Table 2
Process history with phase analyzing in the reinforcement and the matrix.

Process	Course	
	Reinforcement	Matrix
Arrested SHS	TiO_xC_y (enclosing TiO)	
SHS	Bursting of envelope $TiO(C)$, Ti_2O_3 → O, O	
500 °C–8 h	Oxygen outflow from Ti compounds Al_2O_3, $Ti_3O_2(C)$, Ti_2O_3 → O, O	Al_2O_3 formation
1000 °C–1 h	Oxygen outflow and Ti_2O_3 disappearing $Al_{65}Si_{11}Ti_{24}$ ← Si	Formation of Al_3Ti and next $(Al–Si)_3Ti$ Al_2O_3, $Ti_3O_2(C)$ → O
1000 °C–6 h	Alumina encircling on Ti(C) Al_2O_3 (enclosing $Ti(C)$)	Al replaced by Si $Al_{12}Si_{55}Ti_{33}$-τ2

In the presented investigations, to determine the reaction course and its subsequent stages, the microwave field was turned off at the moment of maximum temperature jump. With no support of the synthesis, incompletely processed Ti particles remained. Usually, TiO particles with large voids inside were enveloped with jagged TiO_xC_y compounds, see Fig. 5 and Table 2. With finer Ti particles, phases similar to typical structures produced in complete synthesis were formed. Considering these results, a model of the synthesis course in CO_2 flow is proposed, shown in Fig. 4. In the second stage, CO as a disproportionating agent introduces carbon to TiC_xO_y, replacing oxygen. The synthesis course and type of the components makes this process similar to more widely investigated carbothermal reduction of TiO_2, where CO reduces $Ti_nO_{2n−1}$ to lower oxides (n = 2, 3, 4) and subsequently introduces C to TiC_xO_y compound,

where $0.6 < x < 0.7$ and $0.3 < y < 0.4$ [11,12]. The agent determining the reaction kinetics is concentration of CO that should be 100 times higher than concentration of CO_2 to sustain the process [11,13]. It can be said that the more factors favouring its creation, e.g. developing graphite surface or ball-milling the powders, the more efficiently oxygen will be removed from TiC(O) during the third synthesis stage.

The prepared porous preforms as well as the ball milled Ti–C mixture were subject to XRD analysis. After milling no reaction products were detected, mixture consisted of initial Ti and C powder. In the preforms without graphite, alumina originated from Saffil fibres as well as carbides and oxides were detected, but their peaks superimposed and were difficult to be interpreted unambiguously, see Fig. 6. Phase identify was established
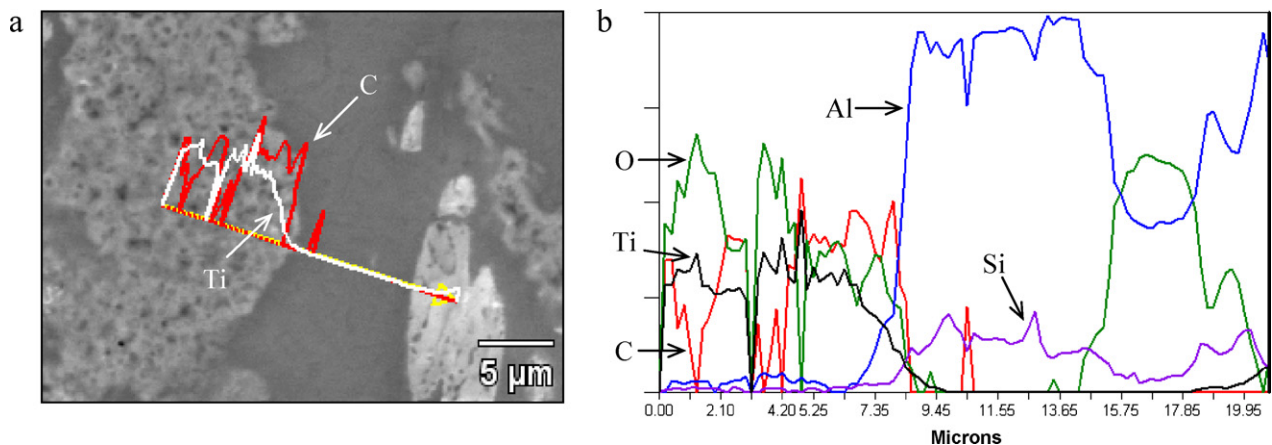

Fig. 9. Linear EDS analysis of (a) Ti compound-matrix interface, with (b) detailed Al, C, O, Si and Ti elements concentration.
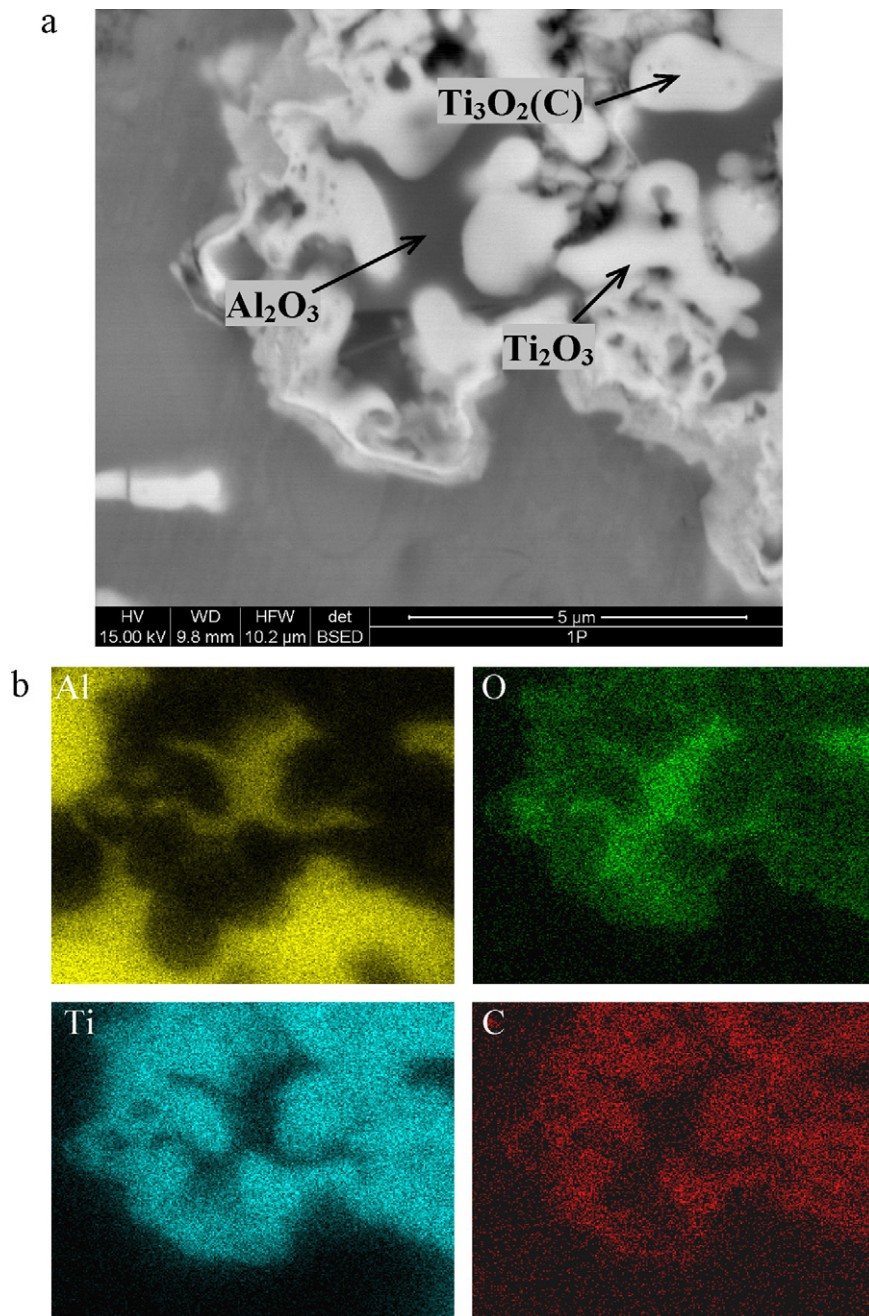
Fig. 10. (a) BSE image with EDS analysis of composite reinforced with the A10T10 preform after annealing at 500 °C for 8 h, and (b) mapping of Al, O, Ti and C elements.

using search-match program with calculation of figure of merit (FoM) values. In the order of best match, the compounds TiC, TiO, TiO_xC_y could be specified. In the latter compound, the coefficient x amounted to 0.32, 0.55 and 0.7, whereas the coefficient y amounted to 0.46, 0.43 and 0.3, respectively. In the synthesized preform containing 10% C, the peaks were intensified and additional reflexes corresponding to graphite occurred. Similar XRD patterns were obtained for all the tested compositions with various Ti and C contents.

Microstructures of the specimens after infiltration with AlSi7Mg aluminium alloy were characterised by sufficient homogeneity, see Fig. 7a. The Ti compounds formed corrugated precipitates composed of finer grains connecting together into closed chains or more compacted colonies. Next to them, a few porosities impermeable for infiltrating aluminium alloy appeared. In the preforms

with preliminary milled graphite and Ti powder, C flakes adhering to Ti-based compounds were observed (Fig. 7b).

Analysis of elements concentration in precipitates showed that Ti was distributed relatively uniformly in the entire volume, whereas in the external areas (lighter) higher concentration of carbon and lower concentration of oxygen occurred. Thus external areas represent titanium oxide with carbon inclusions TiO(C), internal Ti_2O_3 with very small carbon content (Fig. 8, Table 2)

During infiltrating the preforms with liquid aluminium alloy, a limited-due to low temperature-reaction of Al with titanium oxide could occur. Usually initiation of aluminothermic reduction is determined by means of DSC at 830–850 °C [14,15], which can be expressed as:
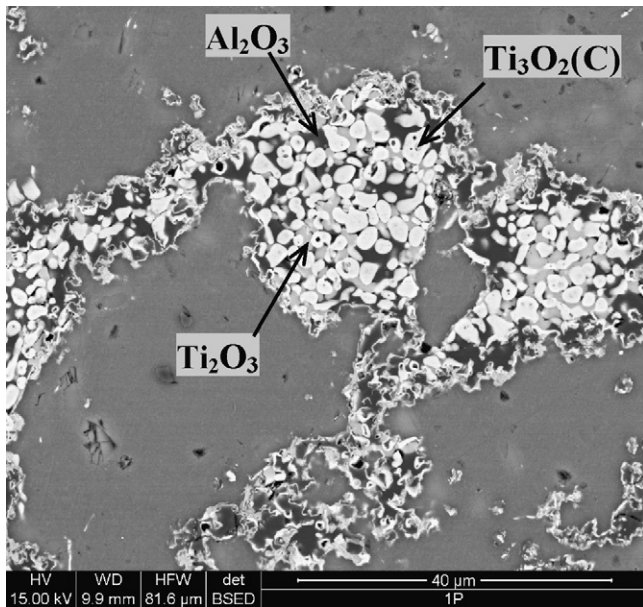
$$3TiO_2 + Al \rightarrow 2Al_2O_3 + Al_xTi_y \qquad (3)$$

Fig. 11. Microstructure of composite reinforced with the A10T10 preform after annealing at 500 °C for 8 h.

Fig. 12. (a) BSE image with EDS analysis of composite reinforced with the A10T10C10 preform after annealing at 1000 °C for 1 h, and (b) mapping of Al, O, Ti and C elements.

3.2. Phase transformation during annealing at 500 °C

It could also proceed as a SHS reaction. In the presented investigation, temperature of 760 °C could be insufficient to initiate the reaction with the infiltrating alloy. However, TEM observations in [16] confirmed the reaction products after saturating a TiO_2–Al_2O_3 ceramic preform at 750 °C. Nanocrystals of β-TiO, β-Ti_2O_3 and α-Al_2O_3 embedded in the Al matrix were detected. Linear analysis at the interface reinforcement-matrix shows gradual concentration changes of Al and Ti, see Fig. 9. Ti atoms are gradually replaced by Al atoms and in the case of Ti_2O_3, Al_2O_3 is formed in its place. Thus, concentrations of Al and Ti change gradually at the interface, whereas concentrations of O and C change abruptly.

3.2. Phase transformation during annealing at 500 °C

The manufactured materials were subjected to annealing at 500 °C for 8 h and during that time structure transformations were observed, especially distribution of elements and formation of distinct phase boundaries. Segregation proceeded in the reinforcement elements: Ti or C and Al or O accumulated in the same areas, see Fig. 10b. Oxygen flew out from created during SHS synthesis TiO(C) to the Al matrix and Al_2O_3 was formed mostly between grains of titanium compound, see Fig. 10a. The composite matrix remained unchanged. In more compact and larger clusters, gray Ti_2O_3 oxides also occurred which in some sense had no time to convert completely, see Fig. 11. Finally, beside unchanged Ti_2O_3 the compound $Ti_3O_2(C)$ more rich in Ti was formed.

3.3. Annealing at 1000 °C

Subsequent annealing at higher temperatures was intended to create stable compounds in the saturated reinforcement and to precipitate new phases in the aluminium matrix. With respect to the process thermodynamics and possible creating new compounds, annealing at 1000 °C for 1 h or 6 h was applied. Further oxygen outflow, segregation in the reinforcement, and forming new phases in the matrix proceeded. After 1-h annealing, decomposition and decay of Ti_2O_3 occurred and thus the reinforcement was composed of $Ti_3O_2(C)$ grains and Al_2O_3 only, see Fig. 12. Titanium released in the reaction (5) usually combines with Al to form Al_3Ti. How-

ever, in [17–19] formation of α2-Ti_3Al was observed first and next of γ-TiAl, that was explained by low solubility of Ti in Al. It could be still found that creation of the final compound is decided by substrate concentration. In the examined materials, Ti passed to the matrix, where it formed plates of $Al_{65}Si_{11}Ti_{24}$. Presumably, it develops by substituting Al atoms by Si atoms in the ordered lattice of Al_3Ti, until the stable $Ti(Al_{0,8}Si_{0,2})_3$ is created. Though, it was found in [16] that after annealing at 650 °C, the compound (Al–Si)$_3$Ti is formed immediately without any intermediate phase. During microscopic investigations, formation of $Al_{65}Si_{11}Ti_{24}$ (corresponding to $Ti(Al_{0,8}Si_{0,2})_3$) was discovered next to Si crystals, where at low solubility of Si the α-solution gets saturated and the compound is formed more quickly. Generally larger Ti based compounds could be found in the composite matrix, as well as tiny but numerous alumina inclusions and rare $Al_{65}Si_{11}Ti_{24}$ plates.

Prolonged annealing for 6 h caused almost complete oxygen outflow from the $Ti_3O_2(C)$ compound and arising rounded grains containing Ti and 12–20% C covered with thin alumina envelope, see Fig. 13. Transformation of the precipitates can be described by the reaction:

$$TiO_2 + 3C + 8Al \rightarrow 4Al_2O_3 + 3TiC + 3Ti, \qquad (4)$$

that is the basic formula for producing TiC–Al_2O_3–Al composites [20–22]. In the examined material, oxygen diffuses to the Al_2O_3
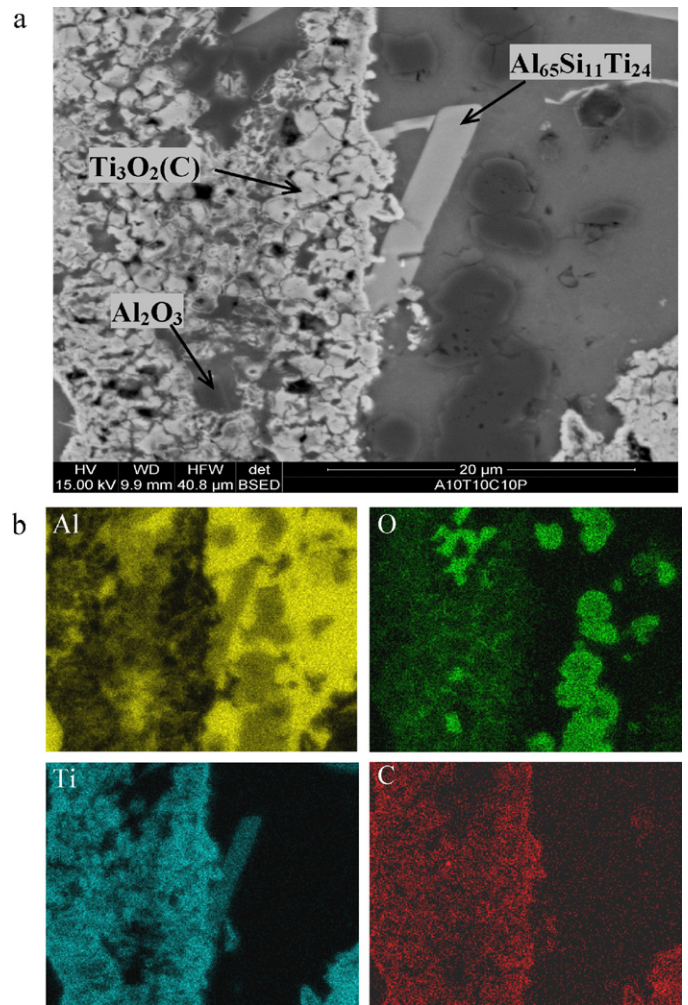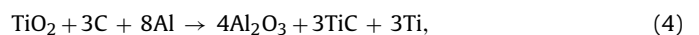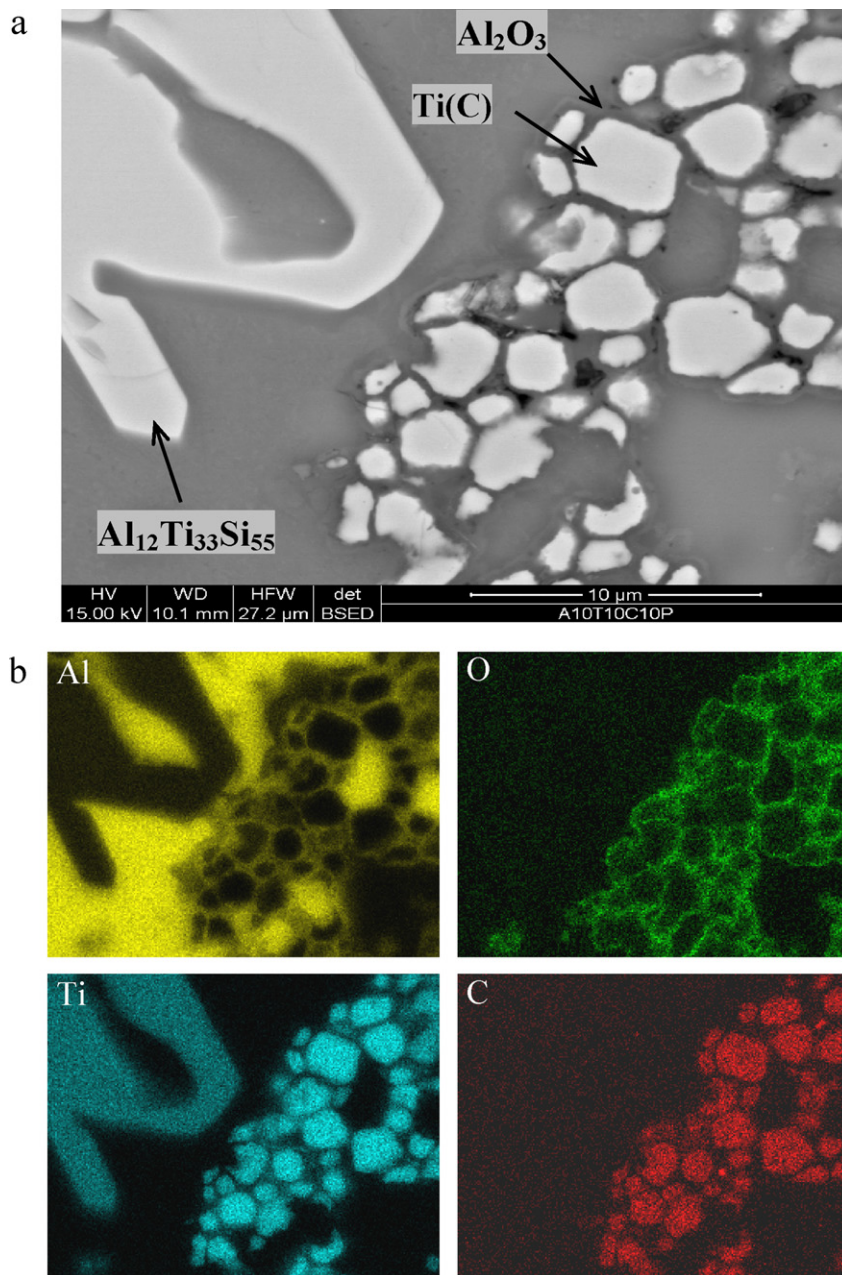
Fig. 13. (a) BSE image with EDS analysis of composite reinforced with the A10T10C10 preform after annealing at 1000 °C for 6 h, and (b) mapping of Al, O, Ti and C elements.

envelope that simultaneously acts as a diffusion barrier for Ti and C. Taking into account the Ti–C system and the finally obtained concentration of C in Ti(C), it could be described as the mixture α-Ti + γ-TiC. As before, Al_2O_3 is present between the reinforcement grains, see Fig. 14. If it accumulates and forms larger clusters, numerous voids are created inside them. This is similar as in [23], where during the reaction of TiO and Al with γ-Al_2O_3, α-Al_2O_3 was formed and porosity in the obtained composite reached 10–15%.

In the matrix, further transport of Si and precipitation of numerous pellets of $Al_{12}Ti_{33}Si_{55}$ proceeded, whose chemical composition and morphology correspond to the phase $\tau 2$ equivalent to Ti_3AlSi_5. It is possible that the peritectic transformation proceeded of $Ti(Al_{0,8}Si_{0,2})_3$ that was formed earlier during annealing for 1 h. As was mentioned before, Si from the matrix dis-

lodged Al atoms whereas the amount of Ti became at the same level.

3.4. Hardness HB of composite materials

Hardness examinations evidenced distinct hardening of the matrix caused by the created titanium compounds. With increasing Ti content from 5% to 10%, average hardness increased to the range between 82 and 99 HB. In turn, increase of graphite content from 5% to 10% (composite reinforced by the A10T10C5 and A10T10C10 preforms) slightly reduced hardness to ca. 85 HB, see Fig. 15. Depending on annealing temperature and time, heat treatment of the composites resulted in various effects. Annealing at 500 °C decreased hardness, whereas annealing at 1000 °C improved the composite properties. The best effect was achieved after
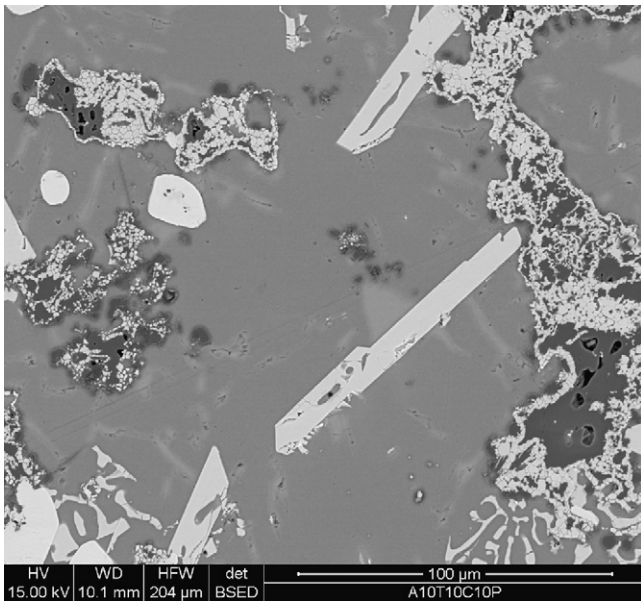
Fig. 14. Microstructure of composite reinforced with the A10T10C10 preform after annealing at 1000 °C for 6 h with created in the matrix $Al_{12}Ti_{33}Si_{55}$ plates.
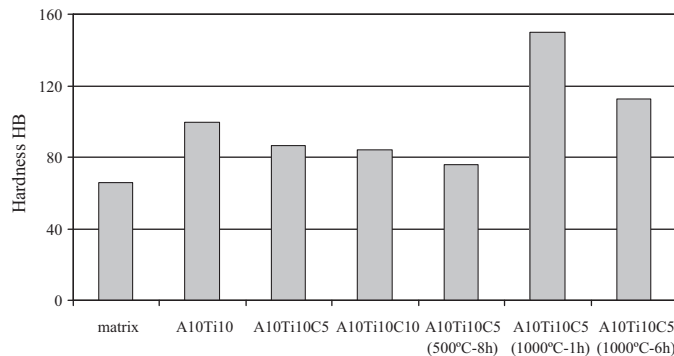

Fig. 15. Hardness HB of the matrix and composites reinforced with the A10T10, A10T10C5, A10T10C10 preforms before and after annealing.

annealing the A10T10C10 specimens for 1 h, when their hardness was ca. 150 HB.

4. Conclusions

Porous preforms of Ti and C powders and Al_2O_3 fibres were produced using SHS synthesis. The highest temperature between 1840 and 1960 °C was observed during synthesis of the preforms containing 10% Ti and 5% C, whereas the highest velocity of the propagation front between 0.32 and 0.43 cm/s occurred when ball-milled powders were used. As a result of the reaction with flowing CO_2, jagged compounds consisting of TiO(C) (titanium oxide with admixture of carbon) and rich in oxygen Ti_2O_3 were produced.

Squeeze casting infiltration led to slight reduction of titanium oxide on the interface with liquid aluminium alloy. The composites were characterized by sufficiently uniform structure with a small number of porosities and good bond between the reinforcement and the matrix.

Annealing of the specimens at 500 °C resulted in oxygen outflow from TiO(C) and formation of Al_2O_3 in vicinity of reduced $Ti_3O_2(C)$. Increasing the temperature to 1000 °C resulted in complete decay of Ti_2O_3 present before annealing and formation of $Ti(Al_{0,8}Si_{0,2})_3$ plates in the matrix. The compound $Ti(Al_{0,8}Si_{0,2})_3$ was probably created by replacing Al atoms by Si atoms in Al_3Ti. Prolonging the annealing time to 6 h ended the reduction process, oxygen transport and formation of Al_2O_3 that enveloped oval grains composed of α-Ti + γ-TiC. In the matrix, larger plates of $\tau2$-Ti_3AlSi_5 developed, rich in Si.

The produced composite materials were characterised by higher hardness, especially when were reinforced with graphite-free preforms. Annealing of the composites for 1 h at 1000 °C significantly increased hardness to 150 HB, two times higher than hardness of the unreinforced matrix alloy.

References

[1] F.-L. Toma, C.C. Stahr, L.-M. Berger, S. Saaro, M. Herrmann, D. Deska, G. Michael, Journal of Thermal Spray Technology 19 (January (1–2)) (2010) 137–147.
[2] R. Debdas, B. Bikramjit, B.M. Amitava, Intermetallic. 13 (July (7)) (2005) 733–740.
[3] W.T. Araya, S.K. Nath, S. Ray, Wear 266 (May (11–12)) (2009) 1082–1090.
[4] J.R. Jokisaari, S. Bhaduri, S.B. Bhaduri, Materials Science and Engineering A394 (2005) 385–392.
[5] Yaodong Liu, Wei Liu, Journal of Alloys and Compounds 440 (1–2) (2007) 154–157.
[6] A. Dudek, Z. Nitkiewicz, Archives of Foundry Engineering 8 (1) (2008) 75–78.
[7] P. Mishra, G. Sethi, A. Upadhyaya, Metallurgical and Materials Transactions B 37 (October (5)) (2006) 839–845.
[8] M. Ignatenko, M. Tanaka, Physica B: Condensed Matter 405 (January (1)) (2010) 352–358.
[9] E. Shafirovicha, S.K. Teoha, A. Varma, Combustion and Flame 152 (January (1–2)) (2008) 262–271.
[10] I.E. Molodetsky, E.P. Vicenzi, E.L. Dreizin, C.K. Law, Combustion and Flame 112 (March (4)) (1998) 522–532.
[11] L.-M. Berger, W. Gruner, E. Langholf, S. Stolle, International Journal of Refractory Metals and Hard Materials 17 (May (1–3)) (1999) 235–243.
[12] Mansour Razavi, M.R. Rahimipour, R. Kaboli, Journal of Alloys and Compounds 460 (July (1–2)) (2008) 694–698.
[13] P. Lefort, A. Maitre, P. Tristant, Journal of Alloys and Compounds 302 (April (1–2)) (2000) 287–298.
[14] Peng Yu, S.C. Zhi Mei, Tjong, Materials Chemistry and Physics 93 (September (1)) (2005) 109–116.
[15] I. Gheorghe, H.J. Rack, Metallurgical and Materials Transactions A 33 (7) (2002 July) 2155–2162.
[16] S. Avraham, P.B.R. Janssen, Nils Claussen, D.K. Wayne, Journal of the European Ceramic Society 26 (13) (2006) 2719–2726.
[17] D. Horvitz, I. Gotman, E.Y. Gutmanas, N. Claussen, Journal of the European Ceramic Society 22 (June (6)) (2002) 947–954.
[18] F. Forouzanmehr NKarimzadeh, M.H. Enayati, Journal of Alloys and Compounds 478 (June (1–2)) (2009) 257–259.
[19] Z. Liu, S. Raynova, D. Zhang, Brian Gabbitas, Materials Science and Engineering: A 449–451 (March) (2007) 1107–1110.
[20] Qiaodan Hu, Peng Luo, Youwei Yan, Journal of Alloys and Compounds 439 (July (1–2)) (2007) 132–136.
[21] Duangduen Atong, E.C. David, Ceramics International 30 (7) (2004) 1909–1912.
[22] G. Golkar, S.M. Zebarjad, J. Vahdati khaki, Journal of Alloys and Compounds 487 (November (1–2)) (2009) 751–757.
[23] J. Pan, J.H. Li, H. Fukunaga, X.G. Ning, H.Q. Ye, Z.K. Yao, D.M. Yang, Composites Science and Technology 57 (3) (1997) 319–325.